SUPPLEMENTARY MATERIALS AND METHODS

Clonal analysis

For clonal analysis the plants were grown in the same conditions as those used for the growth curve. Following heat shock treatment (see below), plants were returned to the growth room and left for 4, 6 or 8 days before imaging. The gynoecia were imaged in water using a Leica DM6000 compound microscope, a Zeiss LSM 5 EXCITER Laser Scanning Confocal Microscope, or the Zeiss LSM 780 Laser Scanning Confocal microscope.

Clones of the *Capsella* and *Arabidopsis* fruit were analysed using Sector Analysis Toolbox implemented in MATLAB (http://www.uea.ac.uk/cmp/research/cmpbio/Sector AnalysisToolbox). The organ outline and individual clones were segmented manually in Image J software. For each fruit project, fruits were warped to a mean fruit shape by placing 50 points around the segmented fruit outlines, with five points following the replum and several reference points. For 300µm there were four reference points, one on each corner of the rectangular shape. For gynoecia larger than 300µm there were seven reference points with two at the base, two where the style met the valves, two on the corners of the style and one at the apex of the style in line with the replum. These placed points were subjected to Procrustes Alignment (Gower, 1975) and normalised for scale. For clones were warped to the corresponding mean shape using a Piecewise Linear Warp (Goshtasby, 1986). The area of clones was calculated from the outline in image J, and the length and width were measured using the line tool in Image J.

Heat shocking plant inflorescences

Pots containing a single plant of either *Arabidopsis* or *Capsella* were covered in Clingfilm. A small cross-shaped hole was pierced through the Clingfilm and the young plant inflorescence (1-3cm in height) was threaded through the hole. The inflorescences were heat-shocked by turning the whole plant upside down in a 37˚C water bath for varying times between 30s and 4min.

Gynoecium growth curves

Capsella plants were grown in a controlled environment room on soil. The plants were standardised by selecting those at a similar stage, for example the plants that had 4 leaves at the same time. Whole inflorescences were collected and fixed for PI staining at two day intervals at about the same time of day starting from 19 to 32 days after sowing. This method was developed from a protocol for staging *Arabidopsis* flower buds: whole inflorescences were PI stained and imaged using OPT. *Arabidopsis* inflorescences were collected and

imaged (Sauret-Gueto et al., 2013).

The timing of the first flower of the main inflorescence was given in exact time in hours after sowing (HAS). The timing for subsequent flowers on the same inflorescence was calculated using the plastochron (timing interval between initiation of successive flower primordia) and the flower position. The plastochron was calculated by counting the number of newly open flowers in a 24h period on 10 inflorescences and averaged over several days. Under these conditions the plastochron of *Capsella* was 4.8h. The position of the individual flowers is the order that the flowers were initiated; so that the first flower on the inflorescence (oldest) would be at position 1, the second flower (second oldest) would be at position 2. Since, the flower at position 2 is initiated one plastochron after the first flower (456 HAS), the timing of the second flower would be 456h + 4.8h = 460.8 HAS.

The length and width along the mediolateral axis of gynoecia were measured using the measuring tool in Volviewer. For later stages, when inflorescences were too large for imaging by OPT, the individual fruits along the inflorescence were imaged using Leica M205C stereo microscope and measured in the Leica LAS V4 software. Gynoecium initiation, 0 days after initiation (0 DAI) was assumed to be when the gynoecium is ~40μm in length which corresponds to 450 HAS.

Supporting Model Description

Basic Factors and Functions

Growth patterns are determined by the pattern of factors distributed over the tissue, termed the canvas (Kennaway et al. 2011). Factors have one value for each segment or vertex of the canvas and are denoted by capital letters in the text. In the equations, factors that are fixed to the canvas are denoted by **i** subscripted with the factor name, while those that propagate through the canvas are denoted by the bold letter **s** subscripted with the factor name. For instance, the mobile factor GPROX is described by $\mathbf{s}_{gprox}$ in the equations. It is assumed that factor levels do not dilute with growth.

Factors may promote growth rates through the linear function *pro*, defined as:

$$\mathrm{pro}(p_f, \mathbf{x}_f) = 1 + p_f \mathbf{x}_f , \qquad (1.1)$$

Where $\mathbf{x}_f$ is a factor, F, and **x** denotes **i** or **s**. p_f is a promotion coefficient for that factor.

Factors may inhibit growth through the function *inh*, denoted as:

$$\mathrm{Inh}(h_f, \mathbf{x}_f) = 1 / (1 + h_f \mathbf{x}_f), \qquad (1.2)$$

Where h_f is a inhibition coefficient for that factor. Values of all coefficients are given in Table S4.

Models

2D fruit models were specified using the growing polarised tissue framework as implemented in the MATLAB application *GFtbox*. Full details are available in Kennaway *et al*. 2011 and *GFtbox* can be downloaded from (https://www.uea.ac.uk/cmp/research/cmpbio/Gftbox). The pattern of deformation depends on growth-modulating factors, whose initial distribution is established during setup (-1 DAI to 0 DAI). Factors have one value for each vertex and values between vertices are linearly interpolated across each finite element. In the models described here, the initial canvas is oriented with regard to the external *xyz*-coordinate system such that the canvas base is parallel to the *xy*-axis and the long axis is parallel to the *z*-axis. The initial gynoecium primordium canvas consists of 2,000 elements and is locally subdivided at 160h at the midvalve generating a mesh of 2960 elements. The initial canvas size is 40µm length and 80µm x 60µm width (value of z=-20µm at the base of the canvas).

Each model has two interconnected networks: the Polarity Regulatory Network (PRN) specifies tissue polarity and hence specified orientations of growth, and the Growth rate Regulatory Network (KRN) determines how factors influence specified growth rates. In total, growth interactions are specified in three equations, one for PRN and two for KRN. These networks determine the specified polarity and growth fields across the canvas. Due to the connectedness of the canvas, this specified growth differs from the resultant growth by which the system is deformed. The time step of each model corresponds to 4h of developmental time. Models take about 20min to run on a CORE^{TM}i7 laptop for 84 steps.

PRN

The models involve growth orientations being established by POLARISER (POL, Fig. S7) propagation from a +organiser, which is expressed at the canvas base in the PROXORG region. The identity factor, PROXORG is fixed at 1 at the base of the canvas (purple line Fig. 4C) and 0 everywhere else. The value of POL is fixed at 1 (b_{pol}), where PROXORG is expressed. POL diffuses according to the equation:

$$\partial \mathbf{s}_{pol}/\partial t = D_{pol}\nabla^2 \mathbf{s}_{pol} - \mu_{pol}\, \mathbf{s}_{pol}\,, \qquad (2.1)$$

where D_{pol} is the diffusion rate and μ_{pol} the decay rate of POL throughout the tissue. Parameter values are given in Table S4. POL distribution is allowed to establish during the setup phase for 6 time steps before the commencement of growth.

POL continues to propagate and the polarity field readjusts according to POL levels throughout growth. The polarity field deforms during growth because changes in tissue geometry affect the way POL becomes distributed.

KRN

There is a basic specified growth rate parallel to the polarity gradient, K_{par} (b_{Kpar}) and a basic specified growth rate perpendicular to the polarity gradient, K_{per} (b_{Kper}) (values in Table S4). The canvas also grows in thickness, K_{knor}, which is maintained at the same rate in all models.

Phases

The timing of the phases was specified by growth factors $\mathbf{i}_{EPHASE}$, $\mathbf{i}_{MPHASE}$ and $\mathbf{i}_{LPHASE}$. $\mathbf{i}_{EPHASE}$ is expressed at 1 everywhere in the canvas ≥ 0h < 48h and 0 after this, $\mathbf{i}_{MPHASE}$ is expressed at a level of 1 everywhere in the canvas at ≥ 48h < 208h (*Capsella*) or 216h (*Arabidopsis*) and 0 before and after this and $\mathbf{i}_{LPHASE}$ is expressed at a level of 1 everywhere in the canvas at ≥ 208h (*Capsella*) or 216h (*Arabidopsis*) and 0 before this.

Model 1 – E Phase and early M Phase (*Capsella* and *Arabidopsis* models)

STYLE and BASE were set up as short gradients (Fig 4D) during the set up phase with a maximum value of 1. During the set up phase the gradients established by propagating from a region of production and then the values were fixed at each vertex once the set up phase was finished. The interactions described in Fig. 4E which set the values for K_{par} and K_{per} can be captured mathematically in the following equations:

$K_{par} = b_{Kpar}$

.pro(p_{EPHASE} , $\mathbf{i}_{EPHASE}$)

.inh(h_{BASE} , $\mathbf{i}_{BASE}$. $\mathbf{i}_{MPHASE}$)

$K_{per} = b_{Kper}$

.inh(h_{STYLE} , $\mathbf{i}_{STYLE}$. $\mathbf{i}_{MPHASE}$)

.inh(h_{BASE} , $\mathbf{i}_{BASE}$. $\mathbf{i}_{MPHASE}$)

$K_{knor} = 0.01$

The basic value of K_{par} is promoted by $\mathbf{i}_{EPHASE}$ and inhibited by $\mathbf{i}_{BASE}$ when $\mathbf{i}_{MPHASE}$ is present. The basic value of K_{per} is inhibited by $\mathbf{i}_{STYLE}$ and $\mathbf{i}_{BASE}$ when $\mathbf{i}_{MPHASE}$ is present. The model was run for 24 time steps (4 DAI).

Model 2 – E and M phase (*Capsella* model)

Model 2 has the same set up as model 1 with the addition of MIDVALVE which is set up as a domain illustrated in Fig. 5C. The interactions described in Fig. 5D which set the values for K_{par} and K_{per} can be captured mathematically in the following equations:

$K_{par} = b_{Kpar}$

.pro(p_{EPHASE} , $\mathbf{i}_{EPHASE}$)

.inh(h_{BASE} , $\mathbf{i}_{BASE}$. $\mathbf{i}_{MPHASE}$)

.pro($p_{MIDVALVE}$, $\mathbf{i}_{MIDVALVE}$. $\mathbf{i}_{MPHASE}$)

$K_{per} = b_{Kper}$

.inh(h_{STYLE} , $\mathbf{i}_{STYLE}$. $\mathbf{i}_{MPHASE}$)

.inh(h_{BASE} , $\mathbf{i}_{BASE}$. $\mathbf{i}_{MPHASE}$)

.inh(h_{REP} , $\mathbf{i}_{REP}$. $\mathbf{i}_{MPHASE}$)

.inh($h_{MIDVALVE}$, $\mathbf{i}_{MIDVALVE}$. $\mathbf{i}_{MPHASE}$)

$K_{knor} = 0.01$

The model was run for 51 time steps (8.5 DAI). During expression of MPHASE the basic value of K_{par} is promoted by $\mathbf{i}_{MIDVALVE}$ and inhibited $\mathbf{i}_{BASE}$. The basic rate of K_{per} is inhibited by $\mathbf{i}_{BASE}$, $\mathbf{i}_{STYLE}$, $\mathbf{i}_{REP}$ and $\mathbf{i}_{MIDVALVE}$ when MPHASE is expressed.

Model 3 – E, M and L phase (*Capsella* model)

GDIST, GPROX and GMIDVALVE were set up as linear gradients and APEX was set up in small patches in the proximal region of the midvalve (Fig. S4). These three factors have a maximum value of 1 and a minimum value of 0. During the set up phase the gradients established through region of production (fixed at 1) and a region of removal (fixed at 0) and then the values were fixed at each vertex once the set up phase was finished. The interactions described in Fig. 6F which set the values for K_{par} and K_{per} can be captured mathematically in the following equations:

$K_{par} = b_{Kpar}$

.pro(p_{EPHASE} , $\mathbf{i}_{EPHASE}$)

.inh(h_{BASE} , $\mathbf{i}_{BASE}$. $\mathbf{i}_{MPHASE}$)

.pro($p_{MIDVALVE}$, $\mathbf{i}_{MIDVALVE}$. $\mathbf{i}_{MPHASE}$)

.inh(h_{BASE} , $\mathbf{i}_{BASE}$. $\mathbf{i}_{LPHASE}$)

.inh(h_{STYLE} , $\mathbf{i}_{STYLE}$. $\mathbf{i}_{LPHASE}$)

.pro($p_{GMIDVALVE}$, $\mathbf{i}_{GMIDVALVE}$. $\mathbf{i}_{LPHASE}$)

.inh(h_{GDIST} , $\mathbf{i}_{GDIST}$. $\mathbf{i}_{LPHASE}$. inh($\mathbf{i}_{APEX}$))

.pro(p_{GPROX} , $\mathbf{i}_{GPROX}$. $\mathbf{i}_{LPHASE}$)

$K_{per} = b_{Kper}$

.inh(h_{BASE} , $\mathbf{i}_{BASE}$. $\mathbf{i}_{MPHASE}$)

.inh(h_{STYLE} , $\mathbf{i}_{STYLE}$. $\mathbf{i}_{MPHASE}$)

.inh(h_{REP} , $\mathbf{i}_{REP}$. $\mathbf{i}_{MPHASE}$)

.inh($h_{MIDVALVE}$, $\mathbf{i}_{MIDVALVE}$. $\mathbf{i}_{MPHASE}$)

.inh(h_{BASE} , $\mathbf{i}_{BASE}$. $\mathbf{i}_{LPHASE}$)

.inh(h_{STYLE} , $\mathbf{i}_{STYLE}$. $\mathbf{i}_{LPHASE}$)

.inh(h_{REP} , $\mathbf{i}_{REP}$. $\mathbf{i}_{LPHASE}$)

.inh($h_{MIDVALVE}$, $\mathbf{i}_{MIDVALVE}$. $\mathbf{i}_{LPHASE}$)

.inh(h_{GPROX} , $\mathbf{i}_{GPROX}$. $\mathbf{i}_{LPHASE}$)

$K_{knor} = 0.01$

The model was run for 84 time steps (9 DAI). During expression of LPHASE the basic value of K_{par} is promoted by $\mathbf{i}_{GMIDVALVE}$ and $\mathbf{i}_{GPROX}$ and inhibited by $\mathbf{i}_{BASE}$, $\mathbf{i}_{STYLE}$, $\mathbf{i}_{MIDVALVE}$ and $\mathbf{i}_{GDIST}$. The basic rate of K_{per} is promoted by $\mathbf{i}_{GDIST}$ and inhibited by $\mathbf{i}_{BASE}$, $\mathbf{i}_{STYLE}$, $\mathbf{i}_{REP}$, $\mathbf{i}_{MIDVALVE}$ and $\mathbf{i}_{GPROX}$ when LPHASE is expressed.

Model 4 – E, M and L phase (*Arabidopsis* model)

The interactions for the *Arabidopsis* model described in Fig. 5H and Fig. 6F, which set the values for K_{par} and K_{per} can be captured mathematically in the following equations:

$K_{par} = b_{Kpar}$

.pro(p_{EPHASE} , $\mathbf{i}_{EPHASE}$)

.inh(h_{BASE} , $\mathbf{i}_{BASE}$. $\mathbf{i}_{MPHASE}$)

.inh(h_{BASE} , $\mathbf{i}_{BASE}$. $\mathbf{i}_{LPHASE}$)

.inh(h_{STYLE} , $\mathbf{i}_{STYLE}$. $\mathbf{i}_{LPHASE}$)

$K_{per} = b_{Kper}$

.inh(h_{BASE} , $\mathbf{i}_{BASE}$. $\mathbf{i}_{MPHASE}$)

.inh(h_{STYLE} , $\mathbf{i}_{STYLE}$. $\mathbf{i}_{MPHASE}$)

.inh(h_{REP} , $\mathbf{i}_{REP}$. $\mathbf{i}_{MPHASE}$)

.inh(h_{BASE} , $\mathbf{i}_{BASE}$. $\mathbf{i}_{LPHASE}$)

.inh(h_{STYLE} , $\mathbf{i}_{STYLE}$. $\mathbf{i}_{LPHASE}$)

.inh(h_{REP} , $\mathbf{i}_{REP}$. $\mathbf{i}_{LPHASE}$)

$K_{knor} = 0.01$

When MPHASE or LPHASE are expressed K_{par} is inhibited by $\mathbf{i}_{BASE}$ and K_{per} is inhibited by $\mathbf{i}_{BASE}$, $\mathbf{i}_{STYLE}$ and $\mathbf{i}_{REP}$. The only difference in growth interactions for LPHASE is that K_{par} is inhibited be $\mathbf{i}_{STYLE}$ when LPHASE is expressed. The model was run for 54 time steps (9 DAI) in Fig. 5 and for 81 time steps (13.5 DAI) in Fig. 6.

Model 5 – E, M and L phase (Spherical model)

The interactions for the Spherical model shown in Supp. Fig. 2 and Fig. 9, which set the values for K_{par} and K_{per} can be captured mathematically in the following equations:

$K_{par} = b_{Kpar}$

.pro(p_{EPHASE} , $\mathbf{i}_{EPHASE}$)

.inh(h_{BASE} , $\mathbf{i}_{BASE}$. $\mathbf{i}_{MPHASE}$)

.inh(h_{BASE} , $\mathbf{i}_{BASE}$. $\mathbf{i}_{LPHASE}$)

$K_{per} = b_{Kper}$

.inh(h_{BASE} , $\mathbf{i}_{BASE}$. $\mathbf{i}_{MPHASE}$)

.inh(h_{STYLE} , $\mathbf{i}_{STYLE}$. $\mathbf{i}_{MPHASE}$)

.inh(h_{REP} , $\mathbf{i}_{REP}$. $\mathbf{i}_{MPHASE}$)

.inh(h_{BASE} , $\mathbf{i}_{BASE}$. $\mathbf{i}_{LPHASE}$)

.inh(h_{STYLE} , $\mathbf{i}_{STYLE}$. $\mathbf{i}_{LPHASE}$)

.inh(h_{REP} , $\mathbf{i}_{REP}$. $\mathbf{i}_{LPHASE}$)

$K_{knor} = 0.01$

The model is run for 48 time steps (8 DAI) in Supp. Fig 2 and 84 time steps (14 DAI) in Fig. 9. When MPHASE and LPHASE are expressed the basic rate of K_{par} is inhibited by $\mathbf{i}_{BASE}$ and the basic rate of K_{per} is inhibited by $\mathbf{i}_{BASE}$, $\mathbf{i}_{STYLE}$ and $\mathbf{i}_{REP}$.

Model 6 – E, M and L phase (Laterally flattened Spheroid model)

The interactions for the laterally flattened Spheroid model (like *Capsella*) shown in Fig. 9, which set the values for K_{par} and K_{per} can be captured mathematically in the following equations:

$K_{par} = b_{Kpar}$

.pro(p_{EPHASE} , $\mathbf{i}_{EPHASE}$)

.inh(h_{BASE} , $\mathbf{i}_{BASE}$. $\mathbf{i}_{MPHASE}$)

.pro($p_{MIDVALVE}$, $\mathbf{i}_{MIDVALVE}$. $\mathbf{i}_{MPHASE}$)

.inh(h_{BASE} , $\mathbf{i}_{BASE}$. $\mathbf{i}_{LPHASE}$)

.inh(h_{STYLE} , $\mathbf{i}_{STYLE}$. $\mathbf{i}_{LPHASE}$)

.pro($p_{MIDVALVE}$, $\mathbf{i}_{MIDVALVE}$. $\mathbf{i}_{LPHASE}$)

$K_{per} = b_{Kper}$

.inh(h_{BASE} , $\mathbf{i}_{BASE}$. $\mathbf{i}_{MPHASE}$)

.inh(h_{STYLE} , $\mathbf{i}_{STYLE}$. $\mathbf{i}_{MPHASE}$)

.inh(h_{REP} , $\mathbf{i}_{REP}$. $\mathbf{i}_{MPHASE}$)

.inh($h_{MIDVALVE}$, $\mathbf{i}_{MIDVALVE}$. $\mathbf{i}_{MPHASE}$)

.inh(h_{BASE} , $\mathbf{i}_{BASE}$. $\mathbf{i}_{LPHASE}$)

.inh(h_{STYLE} , $\mathbf{i}_{STYLE}$. $\mathbf{i}_{LPHASE}$)

.inh(h_{REP} , $\mathbf{i}_{REP}$. $\mathbf{i}_{LPHASE}$)

.inh($h_{MIDVALVE}$, $\mathbf{i}_{MIDVALVE}$. $\mathbf{i}_{LPHASE}$)

When MPHASE and LPHASE are expressed the basic rate of K_{par} is promoted by $\mathbf{i}_{MIDVALVE}$ and inhibited by $\mathbf{i}_{BASE}$ and the basic rate of K_{per} is inhibited by $\mathbf{i}_{BASE}$, $\mathbf{i}_{STYLE}$, $\mathbf{i}_{REP}$ and $\mathbf{i}_{MIDVALVE}$. The model is run for 84 time steps (14 DAI).

Model 7 – E, M and L phase (Medially flattened Spheroid model).

The interactions for the Spherical model shown in Fig. 9, which set the values for K_{par} and K_{per} can be captured mathematically in the following equations:

$K_{par} = b_{Kpar}$

.pro(p_{EPHASE} , $\mathbf{i}_{EPHASE}$)

.inh(h_{BASE} , $\mathbf{i}_{BASE}$. $\mathbf{i}_{MPHASE}$)

.inh(h_{BASE} , $\mathbf{i}_{BASE}$. $\mathbf{i}_{LPHASE}$)

.inh(h_{STYLE} , $\mathbf{i}_{STYLE}$. $\mathbf{i}_{LPHASE}$)

.pro(p_{REP} , $\mathbf{i}_{REP}$. $\mathbf{i}_{LPHASE}$)

$K_{per} = b_{Kper}$

.inh(h_{BASE} , $\mathbf{i}_{BASE}$. $\mathbf{i}_{MPHASE}$)

.inh(h_{STYLE} , $\mathbf{i}_{STYLE}$. $\mathbf{i}_{MPHASE}$)

.inh(h_{REP} , $\mathbf{i}_{REP}$. $\mathbf{i}_{MPHASE}$)

.inh($h_{MIDVALVE}$, $\mathbf{i}_{MIDVALVE}$. $\mathbf{i}_{MPHASE}$)

.inh(h_{BASE} , $\mathbf{i}_{BASE}$. $\mathbf{i}_{LPHASE}$)

.inh(h_{STYLE} , $\mathbf{i}_{STYLE}$. $\mathbf{i}_{LPHASE}$)

.inh(h_{REP} , $\mathbf{i}_{REP}$. $\mathbf{i}_{LPHASE}$)

.inh($h_{MIDVALVE}$, $\mathbf{i}_{MIDVALVE}$. $\mathbf{i}_{LPHASE}$)

When MPHASE and LPHASE are expressed the basic rate of K_{par} is promoted by $\mathbf{i}_{REP}$ and inhibited by $\mathbf{i}_{BASE}$ and the basic rate of K_{per} is inhibited by $\mathbf{i}_{BASE}$, $\mathbf{i}_{STYLE}$, $\mathbf{i}_{REP}$ and $\mathbf{i}_{MIDVALVE}$. The model is run for 84 time steps (14 DAI).

Model 8 – Same as Model 3 except that GDIST activity is removed and K_{par} and K_{per} are inhibited during the late phase.

Diffusion

Details on how diffusion equations are solved can be found in Kennaway et al. (2011). The time steps were chosen to optimise the running time of the model, but the results are the same for smaller time steps. When building the model, the end of the set-up phase was chosen as when the signalling factors that diffused through the canvas had reached an equilibrium. For most factors at this step the diffusion was stopped and so the gradients were established before the growth steps began (e.g. GDIST, GPROX, GMIDVALVE). Fig. S7 depicts the distribution of polariser and the polarity field.

We do not use finite differences, but a finite element method which is capable of stably solving the transient diffusion problem even when 2D dt/dx^2 greatly exceeds 1. It also has the

advantage of not requiring any regularity in the arrangement of the vertices.

The actual values that arise in the simulations are dt = 4, dx = the typical diameter of a finite element = between 1.6 and 6 in the initial state (however, these values increase during growth), and values of D ranging from 0.25 to 15 (all in consistent units). No instability is observed.

Note that the only morphogen that continues to diffuse throughout the simulation is the polariser, with a D of 5, giving 2D dt/dx^2 of 1.1 to 16. Test examples with much larger values of 2D dt/dx^2 show no instability and converge over time to the steady state solution. The other diffusible morphogens only diffuse during the setup phase that establishes the initial conditions of the growth simulation. Their distribution during the final steps of the setup phase indicates that they are near steady state by the beginning of the growth phase.

Models Parameter List

The models parameter list is presented in Supp. Table 1.

SUPPLEMENTARY FIGURES

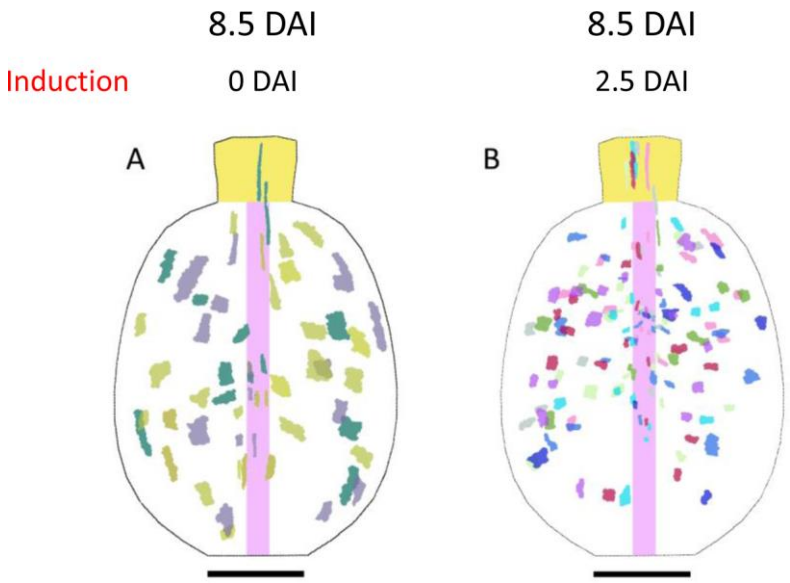

Figure S1. Gynoecium clonal analysis in the middle phase.

(A,B) Sector maps of *Capsella* gynoecium with clones imaged at 8.5 DAI induced at 0 (A) and 2.5 (B). In A, the clones in the valves diverge away from the base and converge back towards the style.

Scale bar, 200µm.

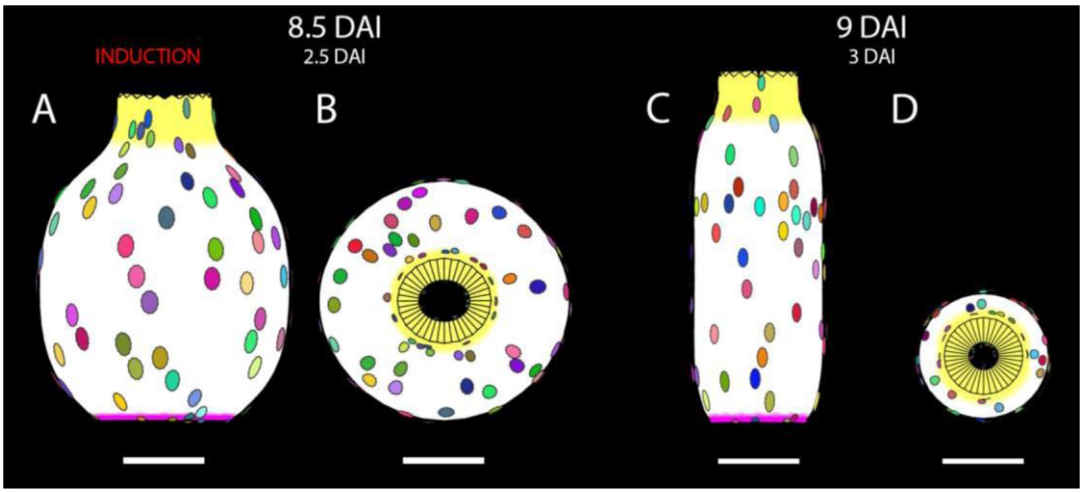

Figure S2. Models with continued growth interactions established in the early phase models.

(A) *Capsella* model outcome at 8.5 DAI showing virtual clone shapes and patterns and (B) cross-section shape is rounded. (C) *Arabidopsis* model outcome at 9 DAI showing virtual clone shapes and patterns and (D) cross-section shape is rounded.

Scale bar 200µm. STYLE, yellow, BASE, pink.

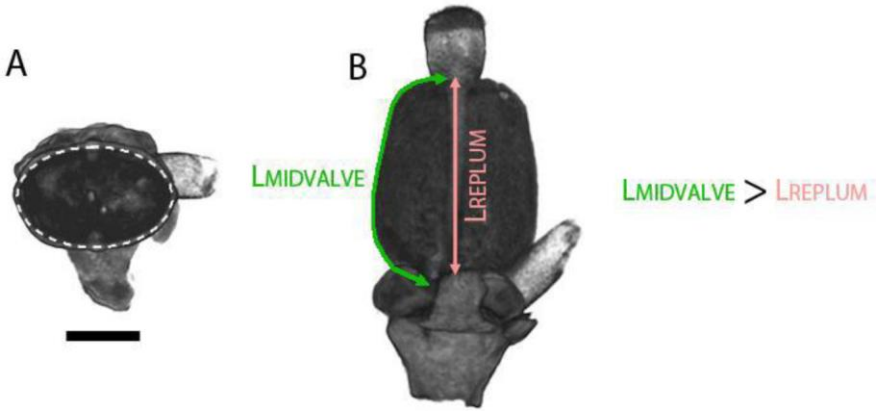

Figure S3. Length of midvalve and replum in *Capsella* gynoecia 8.5 DAI.

(A) Cross section view. White dotted line shows the cross section shape of the gynoecium. (B) Line drawn down the middle of the valve is longer than a line drawn down the replum. Scale bar, 500μm

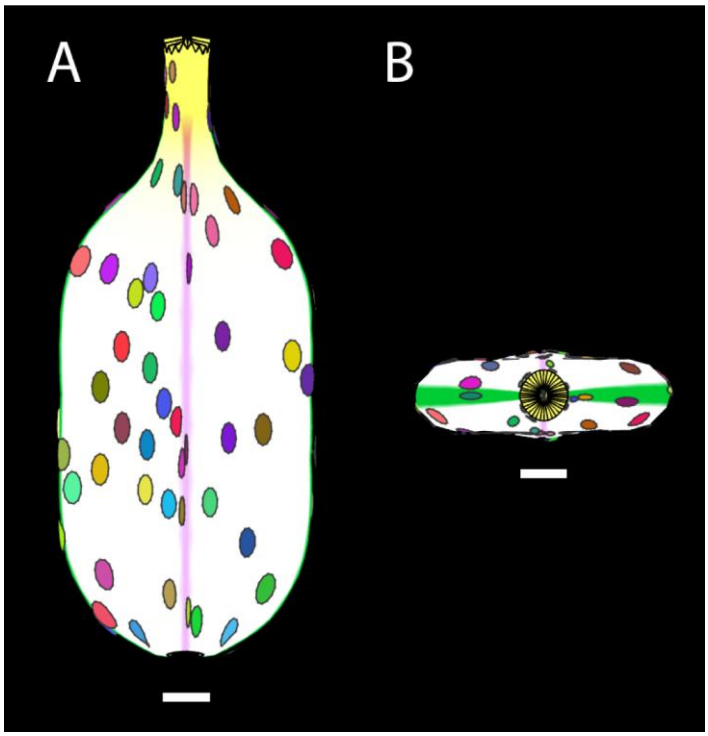

Figure S4. *Capsella* model with continued growth interactions established in the middle phase.

(A) *Capsella* model outcome at 14 DAI showing virtual clone shapes and patterns and (B) cross-section shape. Scale bar 500µm. STYLE, yellow, REP, pink, MIDVALVE, green.

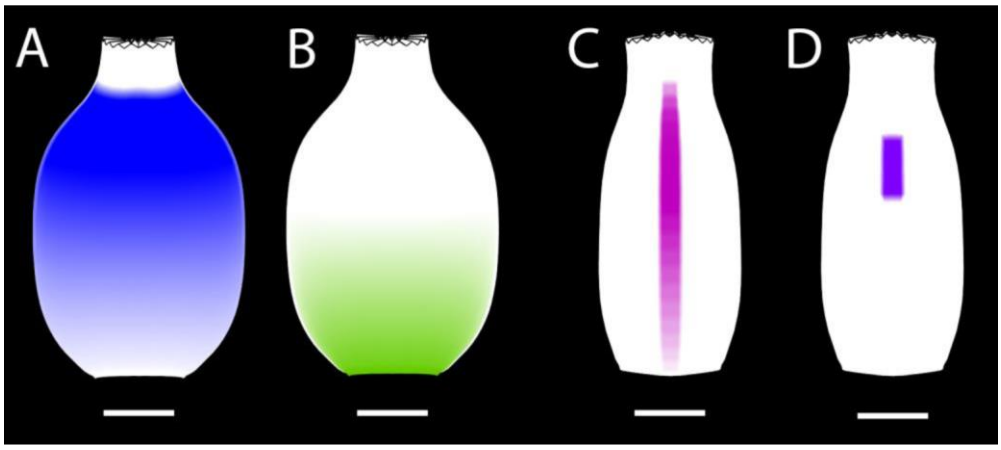

Figure S5. Distribution of Late Phase factors on *Capsella* model at 8 DAI.

(A) GDIST. (B) GPROX. (C) GMIDVALVE. (D) APEX.

Scale bars 200µm.

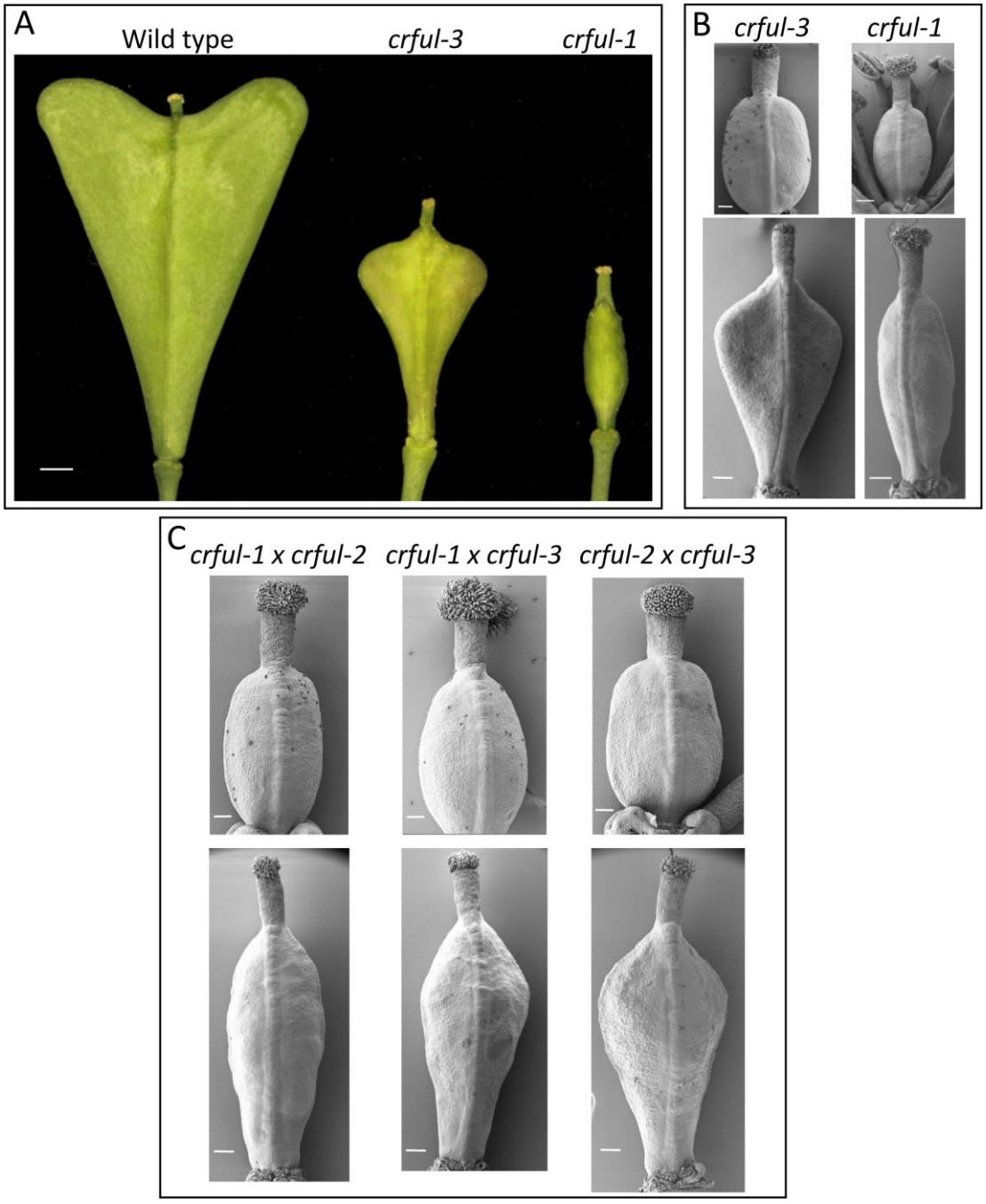

Figure S6. Allelism test of *crful* alleles.

(A) Whole-mount photo of mature fruit from *C. rubella* wild type (left), *crful-3* (centre) and *crful-1* (right). Scale bar, 1 mm.

(B) SEM of fruits from *crful-1* and *crful-3* alleles before (upper) and after (lower) fertilisation. Scale bars, 100 µm (upper), 200 µm (lower).

(C) SEM of fruits from F1 plants originating from the indicated crosses before (upper) and after (lower) fertilisation. See Fig. 2D,G for comparison to wild type at these stages. Scale bars, 100 µm (upper), 200 µm (lower).

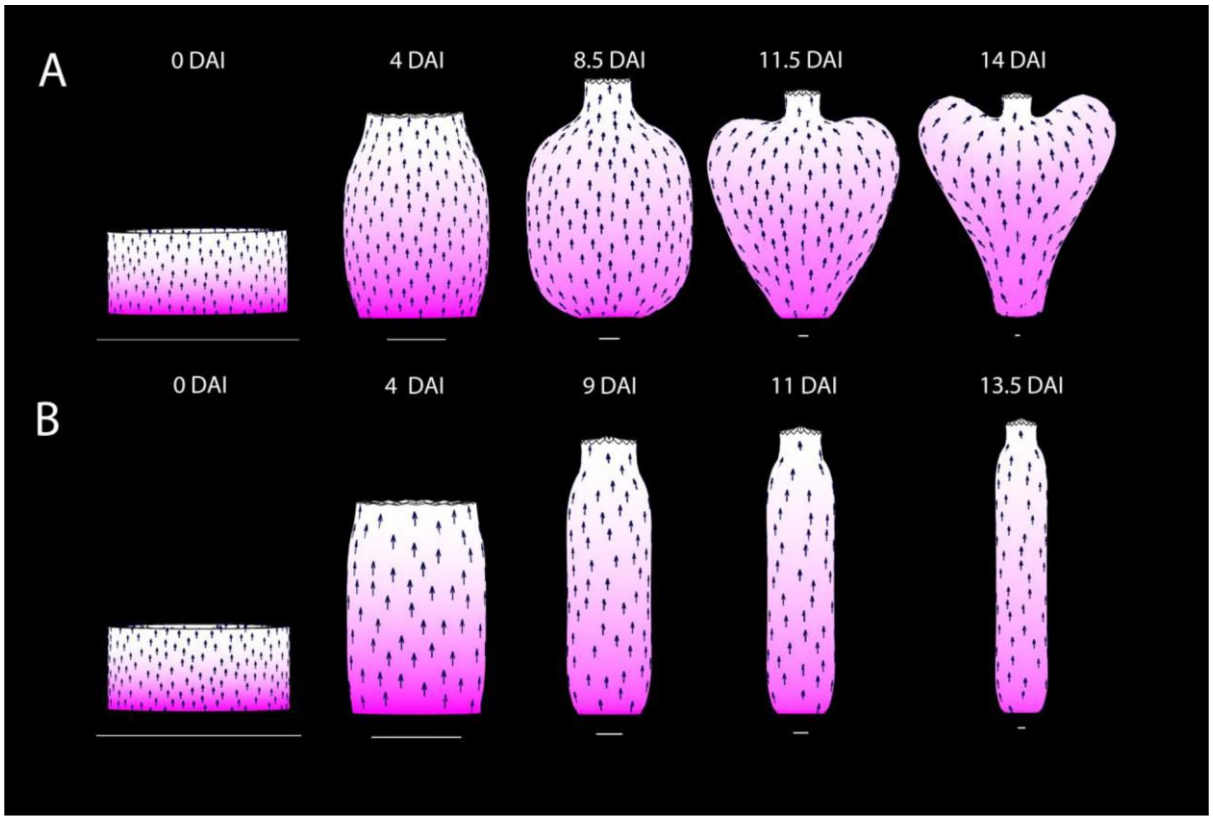

Figure S7. Distribution of POLARISER and orientation of Polarity field on models.
(A) *Capsella* (B) *Arabidopsis.* Scale bars 100µm.

Supplementary Table S1. Cell lengths[1] and widths[2] (µm) in gynoecium of *Capsella* and *Arabidopsis*.

	Capsella 4 DAI		*Capsella* 6.5 DAI		*Arabidopsis* 0 DAI	
	length	width	length	width	length	width
	3.6	9.5	5.5	7.2	4.1	5.3
	4.8	9.7	5.0	8.9	6.6	6.2
	8.2	6.6	8.3	12.5	8.4	7.1
	5.2	4.9	10.3	6.0	6.7	6.5
	5.7	5.6	8.2	7.7	4.0	6.9
	6.1	10.9	5.7	9.6	9.7	5.7
	5.9	7.0	8.2	7.8	5.1	4.8
	7.1	5.2	6.9	8.6	5.7	6.3
	9.6	5.1	7.1	9.6	9.3	5.8
	7.1	4.8	6.8	6.7	5.2	7.6
	7.3	4.8	8.9	9.8	5.1	7.6
	6.5	5.2	6.4	7.2	6.5	7.7
	6.6	6.4	9.7	14.0	6.3	7.8
	9.0	5.3	7.6	11.8	7.4	7.8
	8.7	8.5	8.7	8.5	5.0	8.6
	5.0	7.2	9.2	7.3	5.6	7.7
	3.6	6.8	5.8	15.4	7.2	5.6
	3.8	7.1	5.3	11.9	6.4	7.1
	2.7	7.0	7.9	10.8	7.5	7.8
	2.6	3.4	5.9	9.5	6.4	8.6
	4.7	7.8	6.1	10.1	7.8	8.0
	4.3	7.0	5.7	10.2	8.7	6.2
	3.8	5.9	6.9	8.9	5.5	7.3
	6.3	6.5	11.7	5.5	8.3	7.6
	6.1	6.3	8.9	7.6	8.4	5.6
	7.8	5.4	4.6	7.3	9.6	5.0
	4.7	7.0	5.7	8.3		
	7.9	8.8	4.0	7.1		
	5.9	8.3	3.6	5.8		
	7.7	9.3	4.5	7.1		
	8.2	6.4	6.9	6.7		
	9.0	8.3	8.2	7.5		
	10.1	6.1	8.7	8.2		
	9.6	6.5	5.6	10.1		
	6.0	6.4	5.4	8.1		
	5.9	7.1	7.1	6.6		
	9.9	7.2	4.4	7.6		
	4.5	6.4	6.3	8.4		
	5.6	6.6	6.5	7.5		
	6.8	6.4	4.8	6.9		
	5.6	6.0	5.9	7.6		
	4.3	5.2	5.1	5.8		
	5.8	8.7	6.8	7.6		
	7.9	9.3	7.6	6.6		
	6.9	8.7	8.9	6.3		
	7.8	9.3				
	6.4	4.9				
	10.4	6.2				
	8.1	6.5				
	8.5	6.3				
	5.4	10.1				
	6.3	6.7				
	6.7	6.1				
	6.8	5.3				
	6.1	7.1				
Average	**6.5**	**6.9**	**6.8**	**8.4**	**6.8**	**6.8**
Std deviation	**1.9**	**1.6**	**1.8**	**2.1**	**1.6**	**1.1**
Variance	**3.4**	**2.4**	**3.1**	**4.5**	**2.6**	**1.2**

[1] Cell length was measures parallel to the long axis of the gynoecium

[2] Cell width was measure parallel to the circumferential axis of the gynoecium

Supplementary Table S2. Growth rates of clones (%/hr) during 0-4 DAI of fruit development and model.

	Average	Standard deviation	L/W ratio	Standard deviation	No. clones measured
Capsella					
K_{max}	2.0	0.40	5.4	3.0	8
K_{min}	0.4	0.30			
Model					
K_{max}	1.9	0.26	2.7	0.7	50
K_{min}	0.9	0.16			
Arabidopsis					
K_{max}	2.2	0.44	7.7	3.8	7
K_{min}	0.2	0.26			
Model					
K_{max}	1.7	0.44	3.1	0.8	50
K_{min}	0.6	0.13			

Supplementary Table S3. Growth rates of clones (%/hr) during middle phase* of fruit development and model.

		Mean	Standard deviation	L/W ratio	Standard deviation	No. Clones Measured
Capsella						
Style	K_{max}	1.8	0.06	8.4	0.04	2
	K_{min}	0.3	0.03			
Model	K_{max}	1.1	0.10	3.2	0.60	20
	K_{min}	0.3	0.10			
Replum	K_{max}	0.8	0.20	2.3	0.8	9
	K_{min}	0.3	0.2			
Model	K_{max}	1.1	0.20	2.8	1.0	21
	K_{min}	0.4	0.30			
Valve	K_{max}	1.0	0.27	1.0	0.4	22
	K_{min}	1.0	0.16			
Model	K_{max}	1.1	0.20	1.8	0.8	81
	K_{min}	0.8	0.40			
Arabidopsis						
Style	K_{max}	1.3	0.08	3.1	0.2	5
	K_{min}	0.5	0.06			
Model	K_{max}	1.3	0.10	3.7	0.6	14
	K_{min}	0.3	0.10			
Replum	K_{max}	1.8	0.27	5.7	2.0	5
	K_{min}	0.6	0.17			
Model	K_{max}	1.1	0.35	3.9	1.5	22
	K_{min}	0.2	0.12			
Valve	K_{max}	1.1	0.16	3.0	0.9	10
	K_{min}	0.4	0.16			
Model	K_{max}	1.2	0.30	2.9	0.9	83
	K_{min}	0.5	0.20			

* *Capsella* middle phase clones were induced at 2.5 and imaged at 8.5 DAI and *Arabidopsis* clones were induced at 3 DAI and imaged at 9 DAI.

Supplementary Table S4. Model parameter list.

Parameter	Description	Value
PRN		
Polariser		
b_{pol}	s_{POL} production by $i_{PROXORG}$ (maximum value)	1
D_{pol}	s_{POL} diffusion constant	0.005 mm^2h^{-1}
μ_{pol}	s_{POL} decay rate	0.0001 h^{-1}
KRN		
Basic growth rates		
b_{Kpar}	*Capsella*, spherical, laterally flattened spheroid and medially flattened spheroid models	1.2% h^{-1}
b_{Kper}	*Capsella,* laterally flattened spheroid models	1.2% h^{-1}
b_{Kpar}	*Arabidopsis* model	1.3% h^{-1}
b_{Kper}	*Arabidopsis* model	0.6% h^{-1}
b_{Kper}	medially flattened spheroid model	1.25% h^{-1}
Setting up gradients		
b_{BASE}	S_{STYLE} production by i_{STYLE} (maximum value)	1
D_{STYLE}	s_{STYLE} diffusion rate	0.25 μm^2h^{-1}
b_{BASE}	s_{BASE} production by i_{BASE} (maximum value)	1
D_{BASE}	s_{BASE} diffusion rate	0.25 μm^2h^{-1}
b_{GPROX}	s_{GPROX} production by i_{GPROX} (maximum value)	1
D_{GPROX}	s_{GPROX} diffusion rate	5 μm^2h^{-1}
b_{GDIST}	s_{GDIST} production by i_{GDIST} (maximum value)	1
D_{GDIST}	s_{GDIST} diffusion rate	15 μm^2h^{-1}
$b_{GMIDVALVE}$	$s_{GMIDVALVE}$ production by $i_{GMIDVALVE}$ (maximum value)	1
$D_{GMIDVALVE}$	$s_{GMIDVALVE}$ diffusion rate	15 μm^2h^{-1}
Promotion coefficients		
p_{EPHASE}	growth promotion by i_{EPHASE}	2
$p_{MIDVALVE}$	growth promotion by $i_{MIDVALVE}$	0.2
$p_{GMIDVALVE}$	growth promotion by $i_{GMIDVALVE}$	0.5
p_{GPROX}	growth promotion by i_{GPROX}	2
p_{GDIST}	growth promotion by i_{GDIST}	0.2
p_{REP}	growth promotion by i_{REP}	0.15
Inhibition coefficients		
h_{STYLE}	growth inhibition by i_{STYLE}	3
h_{BASE}	K_{par} inhibition by i_{BASE}	5 (mphase), 100 (lphase)
h_{BASE}	K_{per} inhibition by i_{BASE}	1
h_{REP}	growth inhibition by i_{REP}	5
$h_{MIDVALVE}$	growth inhibition by $i_{MIDVALVE}$	1
h_{GPROX}	growth inhibition by i_{GPROX}	2
h_{GDIST}	growth inhibition by i_{GDIST}	4
h_{APEX}	growth inhibition by i_{APEX}	100